N71-16560

NASA CR-72815
AiResearch 70-7044

PRESSURE CONTAINMENT TESTS
In support of the

NUCLEAR BRAYTON CYCLE HEAT EXCHANGER AND DUCT ASSEMBLY (HXDA)

by

M.G. Coombs, J.C. Gibson, and C.E. Richard

AIRESEARCH MANUFACTURING COMPANY

Prepared for
NATIONAL AERONAUTICS AND SPACE ADMINISTRATION
NASA Lewis Research Center

Contract No. NAS3-13453
P.T. Kerwin, Project Manager

Requests for copies of this report should be referred to

National Aeronautics and Space Administration
Scientific and Technical Information Facility
P. O. Box 33
College Park, Md. 20740

NASA CR-72815
AiResearch 70-7044

TOPICAL REPORT
(PHASE II)

PRESSURE CONTAINMENT TESTS

In support of the

NUCLEAR BRAYTON CYCLE HEAT EXCHANGER AND DUCT ASSEMBLY (HXDA)

by
M.G. Coombs, J.C. Gibson, and C.E. Richard

AIRESEARCH MANUFACTURING COMPANY
Los Angeles, California

Prepared for
NATIONAL AERONAUTICS AND SPACE ADMINISTRATION

January 4, 1971

Contract No. NAS3-13453

NASA Lewis Research Center
Cleveland, Ohio 44135
P. T. Kerwin, Project Manager
Space Power Systems Division

FOREWORD

The studies described herein, which were performed by the AiResearch Manufacturing Company, a division of The Garrett Corporation, were performed under NASA Contract NAS3-13453. The work was done under the direction of the NASA Program Manager, Mr. P. T. Kerwin, Space Power Systems Division, NASA-Lewis Research Center. The AiResearch Program Manager was Mr. M. G. Coombs.

CONTENTS

ILLUSTRATIONS

TABLES

ABSTRACT

The pressure containment capability of plate-fin heat exchangers for nuclear reactor Brayton cycle space power systems were evaluated. Representative plate-fin specimens using 347 stainless steel and Hastelloy X with a nickel base and gold base braze alloy were burst tested at room temperature and 800^0F (700^0K) and creep rupture tested at 1200^0, 1350^0 and 1600^0F (920^0, 1010^0 and 1140^0K).

SECTION I

INTRODUCTION

As part of their advanced space power systems studies, NASA is investigating the performance characteristics of advanced closed loop Brayton cycle electric power generating systems employing liquid-metal-cooled reactors. The heat exchangers associated with this type of power conversion system are the waste heat exchanger, the heat source heat exchanger, and the recuperator. These three heat exchangers and their associated interconnecting ducting define the heat exchanger and duct assembly (HXDA).

To aid in the development of advanced Brayton cycle space power systems, NASA formulated a study to define the associated HXDA heat exchangers and suitable overall packaging configurations. This study was organized in three phases:

Phase I - Parametric Optimization Studies

Phase II - Pressure Containment Tests

Phase III- Preliminary Designs

The Phase I effort was concerned with the selection of basic types of heat transfer surfaces for each of the three system heat exchangers and the development of optimum (i.e., minimum weight) HXDA designs and configurations over a wide range of cycle operating conditions and design variables. The results of these studies are presented in Reference 1. The Phase III studies were directed to the development of two HXDA preliminary designs; one associated with the SNAP-8 reactor temperature capabilities--about 1200°F (920°K) maximum temperature--and the other with a more advanced higher temperature liquid lithium cooled reactor--about 1700°F (1200°K). These two HXDA preliminary designs are presented in Reference 2.

Plate-fin heat transfer matrixes represent an attractive (i.e. light weight and low volume) design approach for both the HXDA-recuperators and waste heat exchangers. In order to obtain data concerning the pressure containment capabilities of plate-fin matrixes operating at the temperature and pressures associated with advanced Brayton cycle systems, NASA formulated a structural test program as Phase II of the HXDA studies. This report summarizes the experimental results obtained in this test program.

SECTION 2

SUMMARY

Burst and creep rupture tests were performed to determine the pressure containment capability of 347 stainless steel and Hastelloy X plate-fin heat exchangers. Representative plate-fin specimens were burst tested at room temperature and 800°F (700°K) and creep rupture tested at 1200°F (920°K), 1350°F (1010°K) and 1600°F (1140°K). The tests, therefore, provide plate-fin pressure capability data over a wide temperature range as shown in Figure 2-1. The data is applicable to a range of fin geometries and design life requirements. A typical strength curve for a 50,000-hr design life using the creep test fin geometry is shown in Figure 2-1.

The tests also provide a strength comparison of plate-fin structures with the nickel base braze alloy, AMS 7-4778, and a gold base braze alloy, Palniro 1. The nickel base alloy has considerably lower cost than the gold alloy and is therefore preferred for fabrication where its use will give satisfactory plate-fin performance. The two alloys will result in different pressure capabilities since their different braze temperature and alloying properties will effect the 347 stainless steel and Hastelloy X fin and sheet strength properties. The pressure capability vs time-to-rupture of the four combinations of parent metal and braze alloy, tested at 1350°F (1010°K), are compared in Figure 2-2. The results show that Hastelloy X brazed with AMS 7-4778 had the highest creep strength although the Hastelloy X-Palniro 1 and 347 stainless steel-AMS 7-4778 types had comparable pressure capability. Although the nickel base alloy had the highest strength at 1350°F (1010°K), the tests also showed that the gold alloy would be preferred at the higher temperatures if corrosion were a design factor.

The plate-fin structure exhibits reductions in pressure capability, as compared to theoretical capability based on fin strength, due to the effects of the fabrication process. Ratios of tested-to-theoretical strength based on parent metal properties varied from 0.41 to 0.83 for the burst tests specimens and 0.51 to 0.85 for creep rupture test specimens. These strength ratios provide design data for use in predicting pressure capability of a wide range of fin geometries and life requirements. However, the data is not strictly applicable to other parent metal or braze alloy combinations and should be considered only as an indication of expected performance of untested alloy-parent metal combinations.

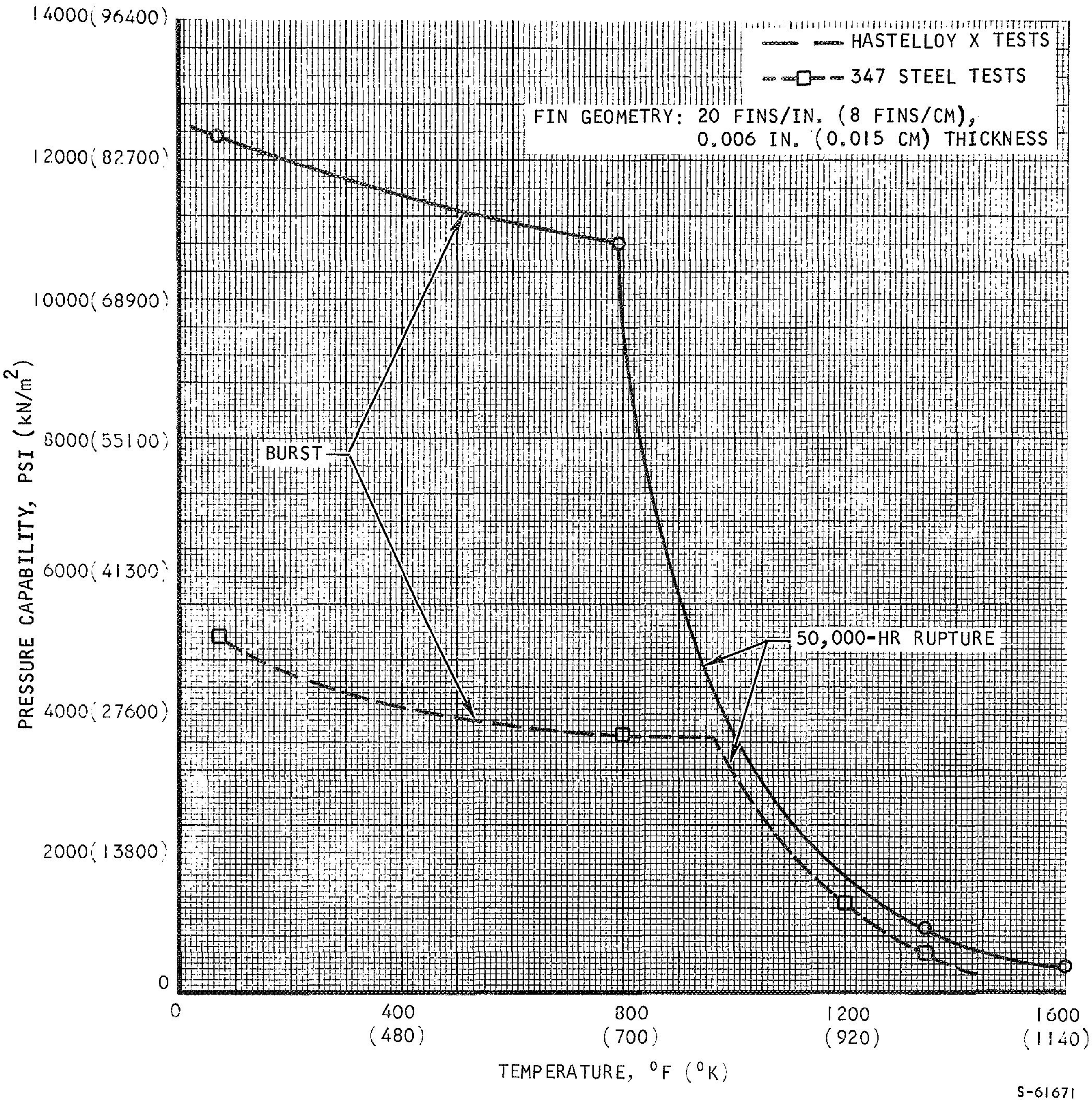

Figure 2-1. Typical Plate-Fin Pressure Capability vs Temperature

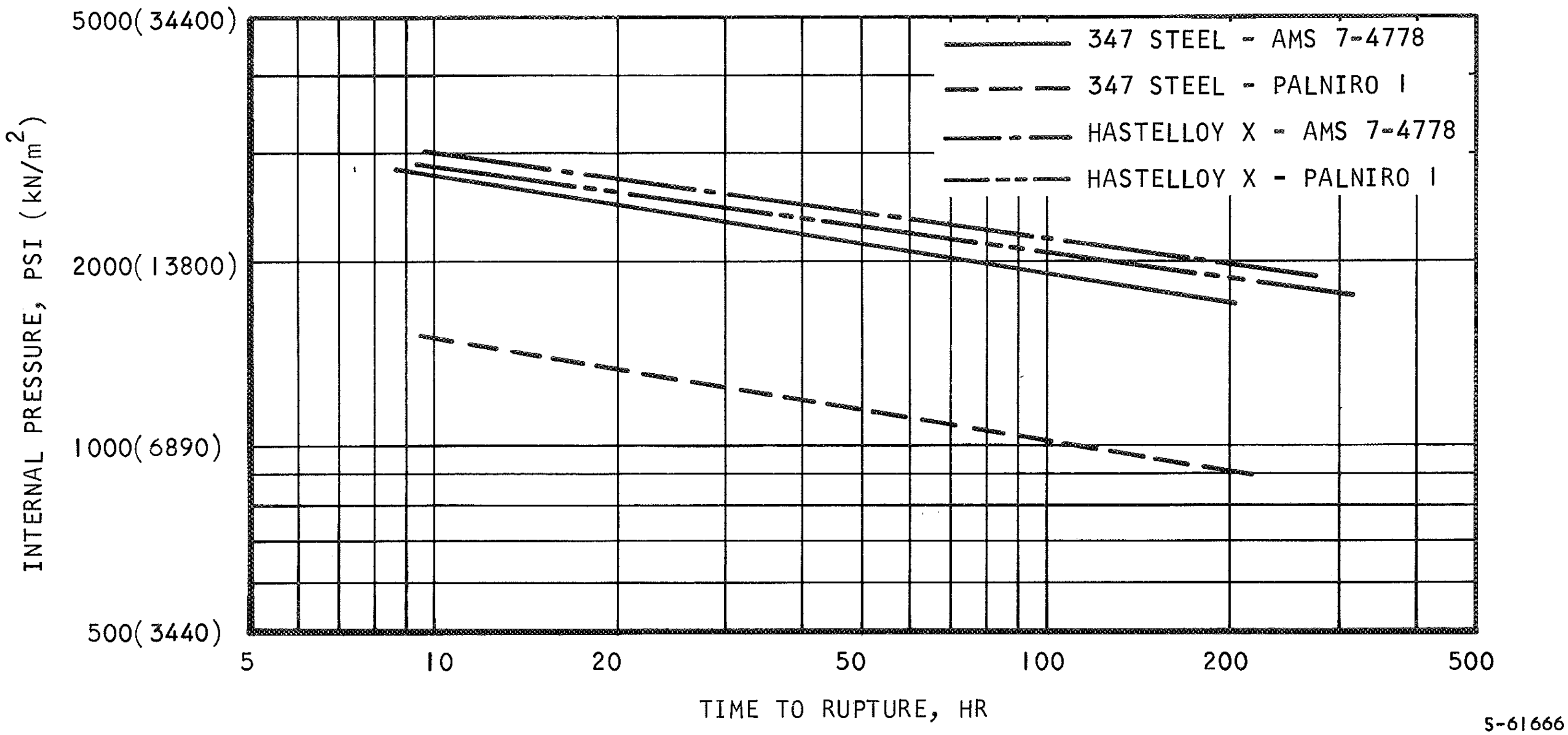

Figure 2-2. Comparative Creep Test Results at 1350°F (1010°K)

SECTION 3

SAMPLE DESIGN AND FABRICATION

The basic pressure containment element in plate-fin heat exchangers is a single-layer sandwich consisting of two sheets and one set of fins. The test specimen was a 3 by 3-in. (8 by 8-cm) section of a single layer enclosed by header bars with a pressurizing tube as shown in Figure 3-1. Photographs of fabricated specimens are shown in Figure 3-2.

FIN GEOMETRY

The rectangular offset fin geometry (shown in Figure 3-1) can be varied to accommodate a range of heat transfer conditions, including the pressure containment requirements. Pressure capability is particularly important for high temperature designs where limited material strength is available and where limitations on maximum fabricable fin densities may be reached. The fin selected for the creep rupture tests was of a relatively high density to be representative of high-temperature requirements and to give conservative strength estimates. The estimates are conservative since as fin density is increased fin shape departs from the desirable square-cornered shape shown in Figure 3-1 and strength reductions are incurred. The creep rupture fin had a 12 percent fin density achieved by having 20 fins/in. (8 fins/cm) with a thickness of 0.006 in. (0.015 cm).

The fin for the burst specimens had a 4.8-percent fin density having 12 fins/in. (5 fins/cm) with a thickness of 0.004 in. (0.010 cm). This lower density fin was used to permit testing at lower pressure levels and also because this fin is more representative of lower temperature operations where creep is not a factor.

Fin heights were 0.18 in. (0.46 cm) for the burst specimens, 0.075 in. (0.19 cm) for 347 stainless steel creep specimens, and 0.05 in. (0.13 cm) for the Hastelloy X creep specimens. Fin height is not an important factor in determining pressure strength since height only effects fin load redistribution capability, primarily in the plastic strain region. The selected heights are typical for the expected design requirements of Brayton cycle power systems.

SHEET THICKNESS

The face sheets with 0.025-in. (0.06-cm) thickness were selected to avoid load transfer from the center of the specimen to the edges and to be representative of minimum heat exchanger side plate thicknesses. The sheet thickness selected had a minor effect on pressure containment capability. Sheet thickness is related to pressure containment capability by its effect on the magnitude of the bending stress due to the unsupported length between fins and due to the ability of the sheet to transfer load from the weaker to the stronger fins. It was estimated that fin load reductions at the center of the specimen due to sheet stiffness would be less than 1 percent. The face sheet bending stresses were a maximum of about 20 percent of the fin stress so that the sheets would not influence containment strength.

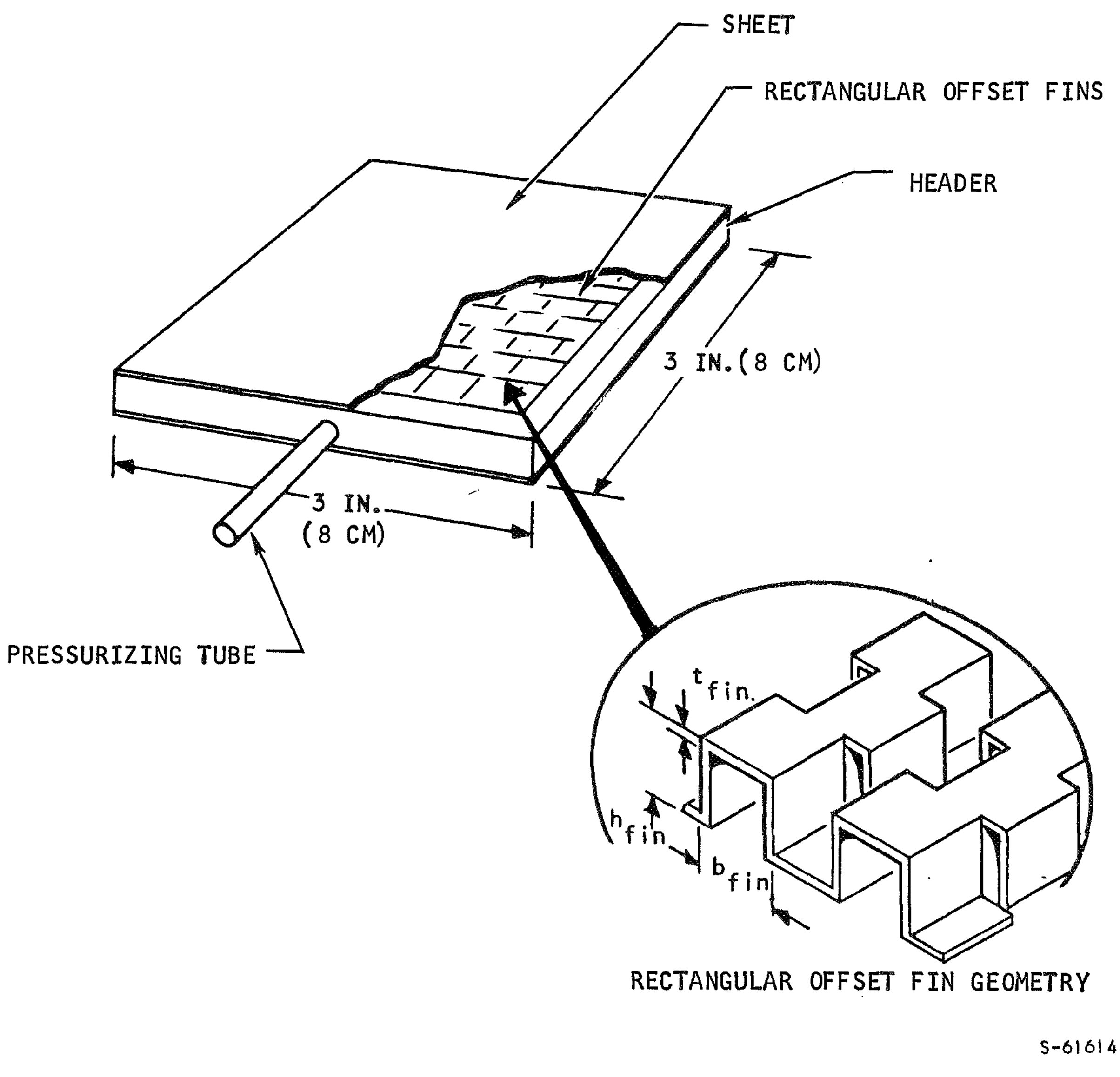

Figure 3-1. Test Specimen

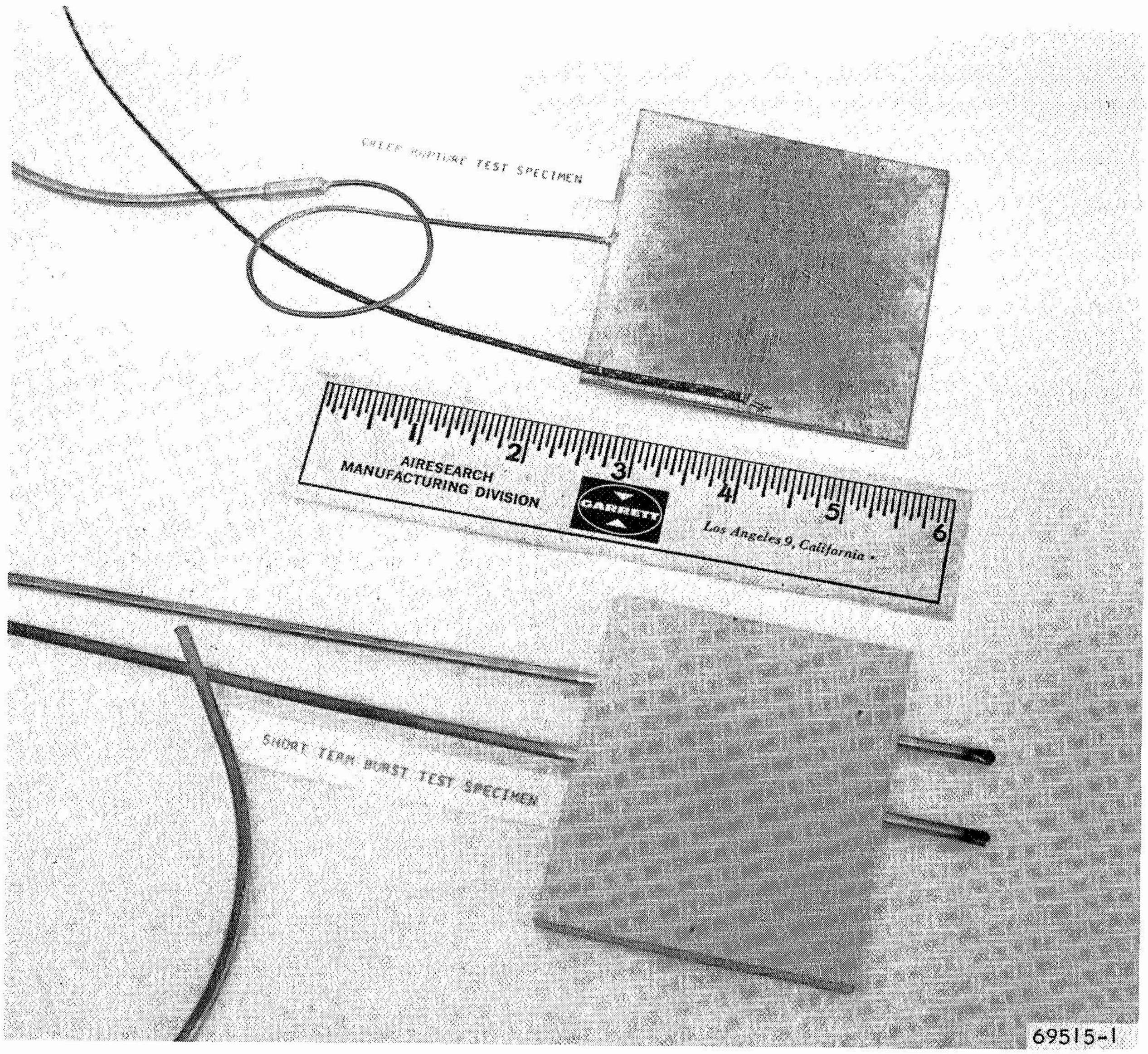

Figure 3-2. Burst and Creep Rupture Specimens

BRAZE ALLOY SELECTION

A nickel-base braze alloy and a gold-base braze alloy were used to illustrate comparative strengths of typical alloys. The nickel base alloy was AMS 7-4778 with the following percentage composition: 92 Ni, 3B, 4.5 Si, and 0.1 C (maximum). The gold-base alloy was Palniro I (50 Au, 25 Pd, 25 Ni). The brazing temperatures for the nickel-base and gold-base alloys were 1975° and 2070°F (1350° and 1410°K), respectively.

FABRICATION

The basic sample was fabricated in a single brazing operation with a 2 to 5 psi (14 to 34 kN/m^2) loading applied to the 3- by 3-in. (8- by 8-cm) surface. Prior to brazing, the AMS 7-4778 alloy (which is in powder form) was applied on the sheets to a depth of about 0.003 in. (0.008 cm) whereas Palniro I foil of 0.001 in. (0.003 cm) thickness were placed between the sheets and fins. The specified time at braze temperature was 0.25 hr to simulate actual recuperator fabrication. An additional braze cycle was required in some cases for the pressurizing tube and to repair leaks at the sheet-to-header bar joint. A lower melting point alloy, Nioro (82 Au, 18 Ni), was used for the additional braze operations that were performed at 1800°F (1260°K).

The creep rupture specimens were pressure tested at room temperature prior to placement in the test furnace to verify sample integrity. Test pressures were 1500 psi (10300 kN/m^2) for 347 stainless steel specimens and 2000 psi (13800 kN/m^2) for Hastelloy X specimens. In selected cases, the samples were repaired to obtain panel integrity for the room temperature proof pressure tests.

SECTION 4

TESTS

Figure 4-1 is a schematic representation of one of the two furnaces used for the creep rupture tests. The two furnaces, with inside dimensions of 10 by 10 by 24 in. (25 by 25 by 61 cm) were each capable of handling six panels and two pressure levels. One furnace had a pressure capability of 2000 to 3000 psi (13800 to 20700 kN/m^2) and the other of 3000 to 5000 psi (20700 to 34400 kN/m^2). The four groups of three specimens were each supplied with a separate pressure system. The specimens were pressurized from a high pressure argon bottle through a regulator and an orifice. The orifice permitted sufficient argon flow to maintain pressure in the advent of small leaks occuring in the system. On specimen failure the orifice restricted the argon flow, and the decreased downstream pressure activated the low pressure alarm. A thermocouple was attached to each speciman and temperatures were recorded periodically. A continuous record was taken of the furnace control temperature. A separate low temperature alarm was incorporated for additional system protection. The specimens were placed in a Hastelloy X rack which separated them so that the failure of one panel would not effect the life of an adjoining panel. Figure 4-2 shows a furnace with six panels installed.

The room temperature burst specimens were connected to a hydrostatic pressurizing system after trapped air was removed from the panels. Hydrostatic pressure was slowly increased until panel rupture occurred as evidenced by a sudden decay in panel pressure or deformation of the panel itself. A ruptured specimen is shown in Figure 4-3. The 800°F (700°K) burst specimens were connected to the argon supply on the high pressure furnace. Temperature was monitored by a thermocouple attached to the panel, while pressure was being gradually increased until rupture occurred. Pressurizing time was 1 to 2 min. The panel was then removed from the furnace for visual examination.

The creep rupture test specimens were instrumented with a fiberglass insulated Cr-Al thermocouple that was attached to the 0.025-in. (0.064-cm) sheet of the panel prior to placement in the furnace. Upon temperature stabilization the panel was pressurized to its selected test pressure. The panel temperature and pressure were monitored at specific intervals and recorded to insure that the correct panel temperature and pressure were being maintained. Temperature and pressure variations were $\pm 10°F$ and ± 1 percent, respectively. A typical creep rupture specimen failure is shown in Figure 4-3.

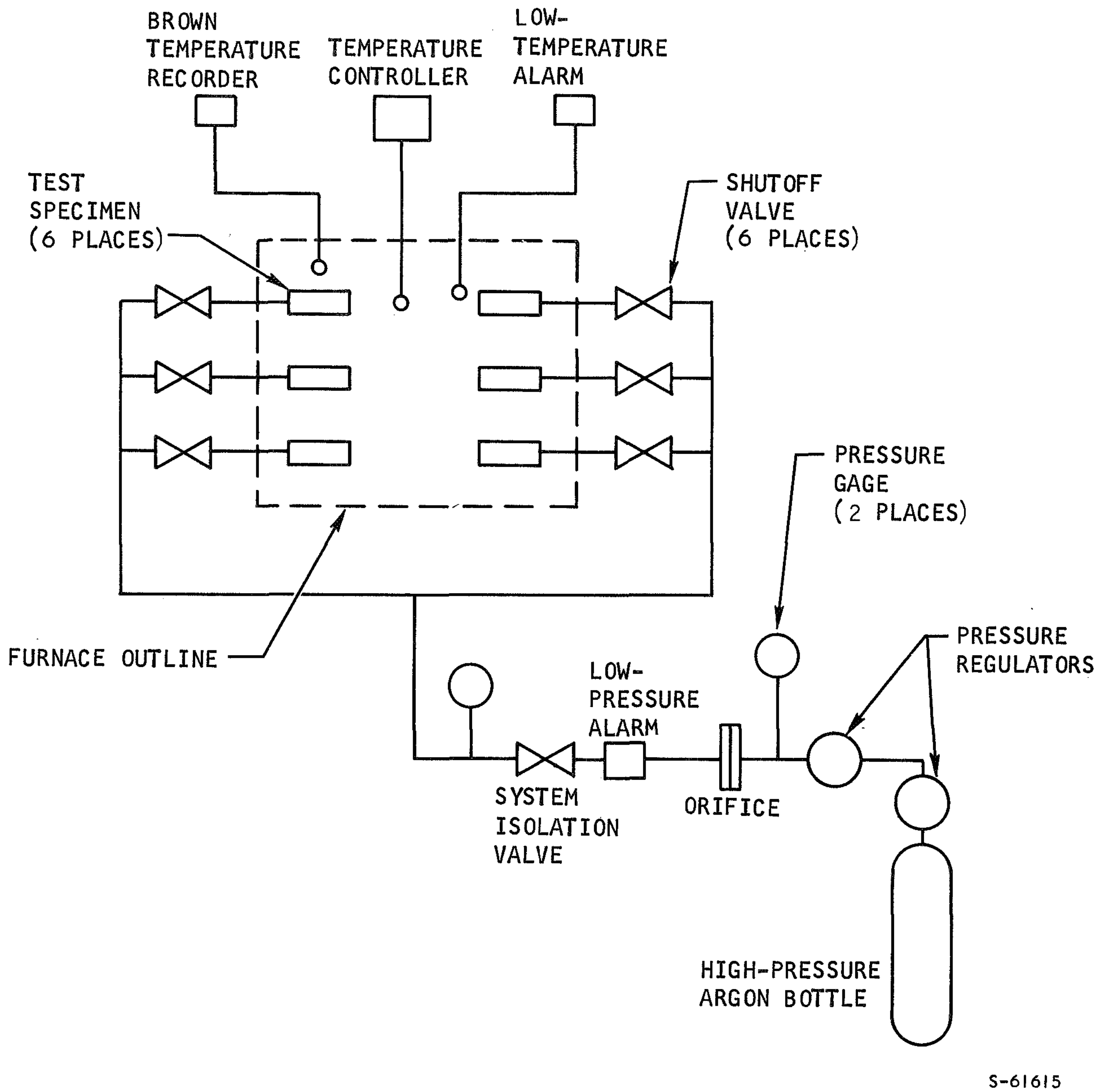

Figure 4-1 Pressure Test System Schematic

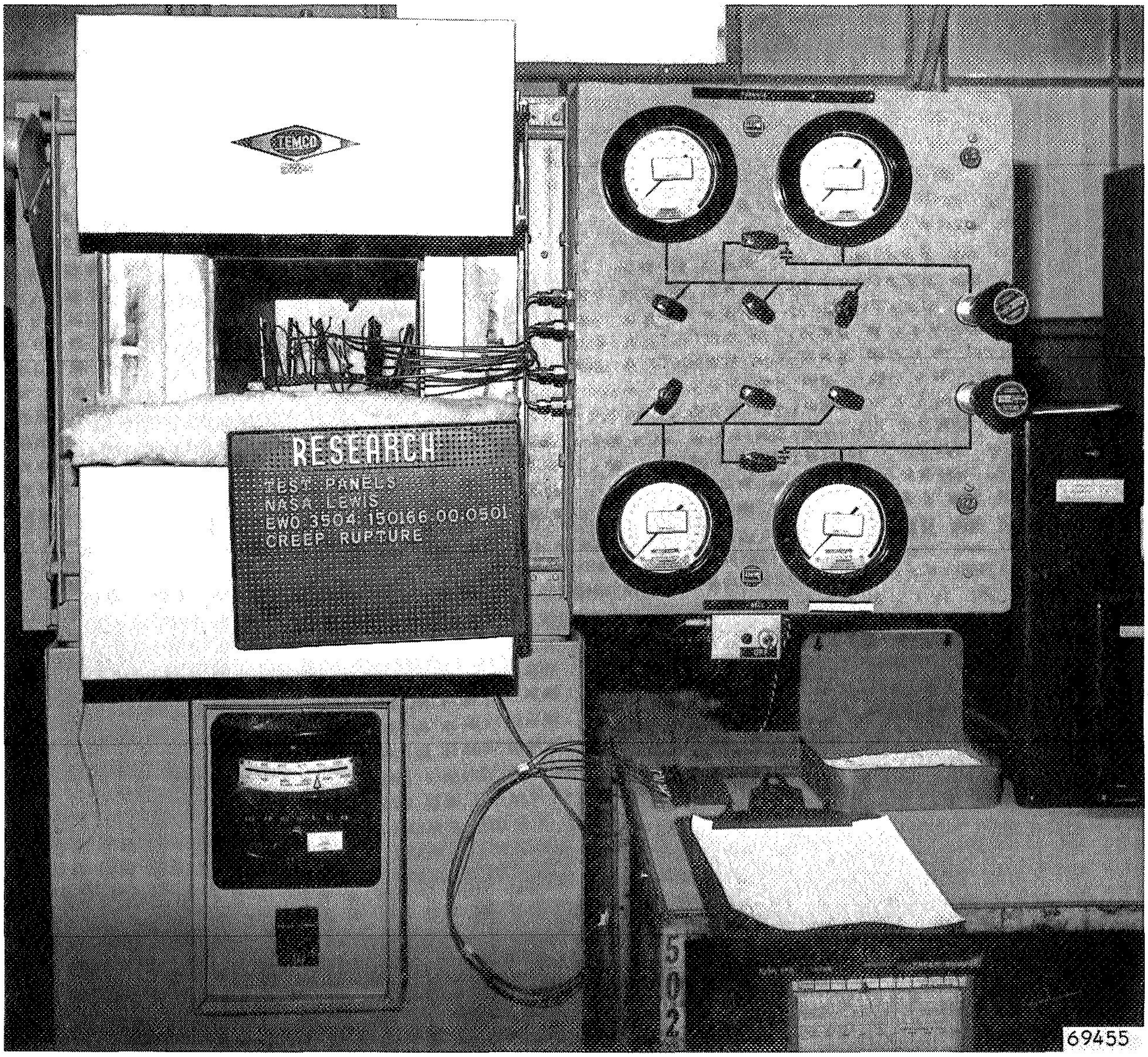

Figure 4-2. Furnace Setup with Test Specimens Installed

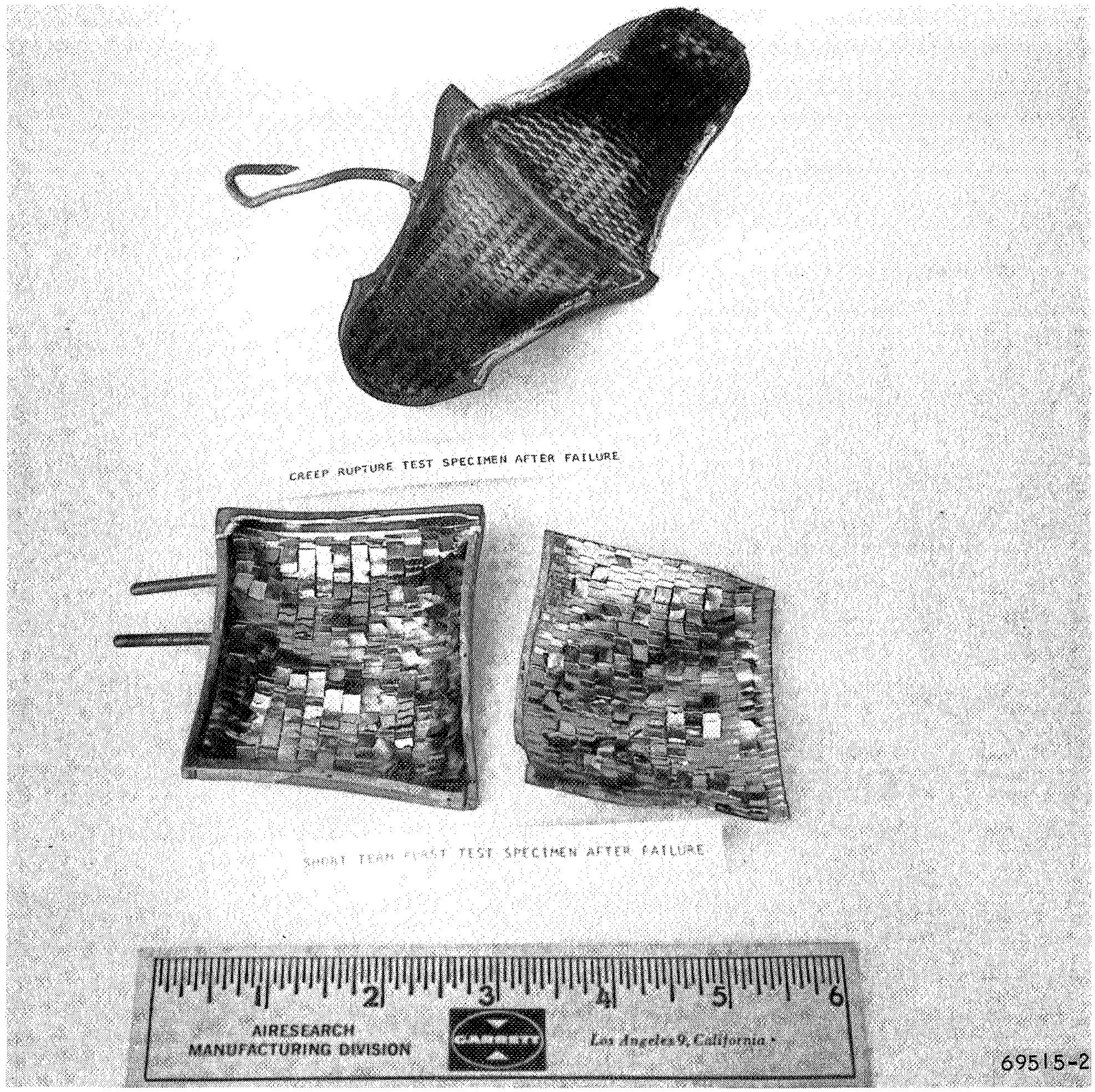

Figure 4-3. Typical Creep Rupture and Burst Specimen Failures

SECTION 5

RESULTS AND DISCUSSION

The pressure containment test results for burst and creep rupture are summarized in Tables 5-1 and 5-2, respectively. The average test values are also compared to estimated fin pressure containment capability assuming a fully effective fin and using published parent metal strength properties of 347 stainless steel and Hastelloy X (References 3 and 4). The resulting strength ratios for the plate-fin structure, which ranged from 0.41 to 0.83 for burst and 0.51 to 0.85 for creep rupture, represent the overall effects of the plate-fin fabrication process on the theoretical fin pressure capability. Plate-fin pressure capability vs temperature can be determined from the test results as illustrated in Figure 5-1. The curves use the test results for 347 stainless steel brazed with AMS 7-4778 and for Hastelloy X brazed with Palniro 1. The curves show the published parent metal burst and 50,000-hr creep rupture strengths. The curves are shown for the 20 fins/in. (8 fins/cm), 0.006-in. (0.015-cm) thickness fin geometry, although similar curves could be constructed for a wide range of geometries to provide design data for plate-fin heat exchangers.

For this test data to be useful to the designer a means of correlating tests such as those conducted in this evaluation with other plate fin geometries is desired. The applied pressure is not a true measure of the severity of the loading on this structure since fin geometry and, to a lesser extent, face sheet geometry can be widely varied to improve or reduce the plate fin internal pressure strength. The simplest means of expressing the loading level devised to date is the fin tensile stress, given by the following:

$$\sigma_{fin} = \text{load/fin area}$$

The theoretical relation between fin stress and pressure, P, is therefore

$$\sigma_{fin} = P(b_{fin}-t_{fin})/t_{fin} \qquad (5\text{-}1)$$

where b_{fin} and t_{fin} are the spacing and thickness, respectively. The above relation is modified to account for actual fin performance by including the strength factor, f, as a correlating factor between pressure and fin stress at failure. Therefore

$$P_{rupture} = f\sigma \left[t_{fin}/(b_{fin}-t_{fin})\right] \qquad (5\text{-}2)$$

where σ is now the material strength capability, either for burst or creep rupture.

TABLE 5-1

BURST TEST RESULTS

Panel Type	Temperature, °F (°K)	Burst Pressure, psi (kN/m²)			Average Strength Ratio (2)
		Test Values	Average Test Value	Metal Strength (1)	
347 Steel-AMS 7-4778	Room Temperature	1870(12900) 1840(12700) 1900(13100)	1870(12900)	4550(31500)	0.41
	800(700)	1330(9160) 1405(9670) 1370(9440)	1370(9440)	3280(22600)	0.42
347 Steel-Palniro I	Room Temperature	2110(14500) 2130(14700) 2140(14700)	2130(14700)	4550(31500)	0.47
	800(700)	1600(11000) 1625(11200) 1700(11700)	1640(11300)	3280(22600)	0.50
Hastelloy X-AMS 7-4778	Room Temperature	3540(24400) 3610(24900) 3280(22600)	3480(24000)	5750(39600)	0.61
	800(700)	3160(21800) 3000(20600) 3310(22800)	3160(21800)	5040(34700)	0.63
Hastelloy X-Palniro I	Room Temperature	4700(32400) 4750(32500) 4860(33500)	4770 (32800)	5750(39600)	0.83
	800(700)	3700(25500) 3700(25500) 3900(26800)	3770(26000)	5040(34700)	0.75

NOTE: (1) Based on nominal fin geometry; 12 fins/in. (5 fins/cm), 0.004 in. (0.010 cm) thickness, $P_{burst} = 0.505\ \sigma_{ultimate}$

(2) Ratio of average test burst pressure to estimated burst pressure based on parent metal strength.

TABLE 5-2

CREEP TEST RESULTS

Material	Braze Alloy	Test Temperature, °F(°K)	Test Pressure, psi (kN/m²)	Time to Rupture, hr	Average Strength Ratio (1)
347 Stainless Steel	AMS 7-4778	1200(920)	3000(20700)	81.9	0.81
			3000(20700)	90.1	
			3000(20700)	164.8	
			2400(16500)	166.0	
			2400(16500)	212.7	
		1350(1010)	2500(17200)	4.8	0.85
			2400(16500)	3.9	
			2400(16500)	12.8	
			2400(16500)	14.4	
			2000(13800)	46.2	
			2000(13800)	47.8	
			2000(13800)	60.5	
			1600(11000)	55.1	
			1600(11000)	62.1	
			1100(7580)	722.0 (2)	
	Palniro I	1200(920)	3300(22700)	3.0	0.58
			3300(22700)	8.3	
			3300(22700)	9.1	
			2600(17900)	20.0	
			2600(17900)	25.3	
			2600(17900)	25.8	
			1800(12400)	60.0	
			1800(12400)	62.3	
		1350(1010)	2000(13800)	1.3	0.53
			2000(13800)	1.3	
			2000(13800)	3.0	
			2000(13800)	3.7	
			1650(11400)	4.3	
			1650(11400)	4.7	
			1500(10300)	7.5	
			1500(10300)	8.5	
			1500(10300)	10.2	
			1100(7580)	32.9	
			1100(7580)	36.8	
Hastelloy X	AMS7-4778	1350(1010)	3500(24100)	3.1 (3)	0.62
			3000(20700)	7.3	
			3000(20700)	8.0	
			3000(20700)	14.8	
			2700(18600) (4)	15.8	
			2400(16500) (4)	22.7	
			2100(14500)	656.6 (2)	
		1600(1140)	1200(8260)	6.0	0.51
			1200(8260)	6.6	
			1200(8260)	7.1	
			1000(6890)	9.4	
			600(4130)	43.1	
			600(4130)	79.0	
	Palniro I	1350(1010)	3000(20700)	8.7	0.59
			3000(20700)	15.3	
			3000(20700)	20.1	
			2700(18600)	10.2	
			2100(14500)	39.3	
			2100(14500)	103.6 (2)	
			1800(12400)	84.0	
		1600(1140)	1300(9850) (4)	3.0	0.59
			1300(8950) (4)	4.3	
			1200(8270	3.6	
			850(5840)	59.2	
			850(5840)	193.3	

NOTES: (1) Ratio of test pressure to estimated pressure which would give equal rupture life using parent metal creep properties, based on 20 fins/in. (8 fins/cm), 0.006-in. (0.015-cm) thickness fin geometry

(2) Test terminated prior to specimen failure

(3) Does not include an additional 10 hr at 3000 psi (20700 kN/m)

(4) Burst specimen; actual test pressure was 0.37 times this pressure

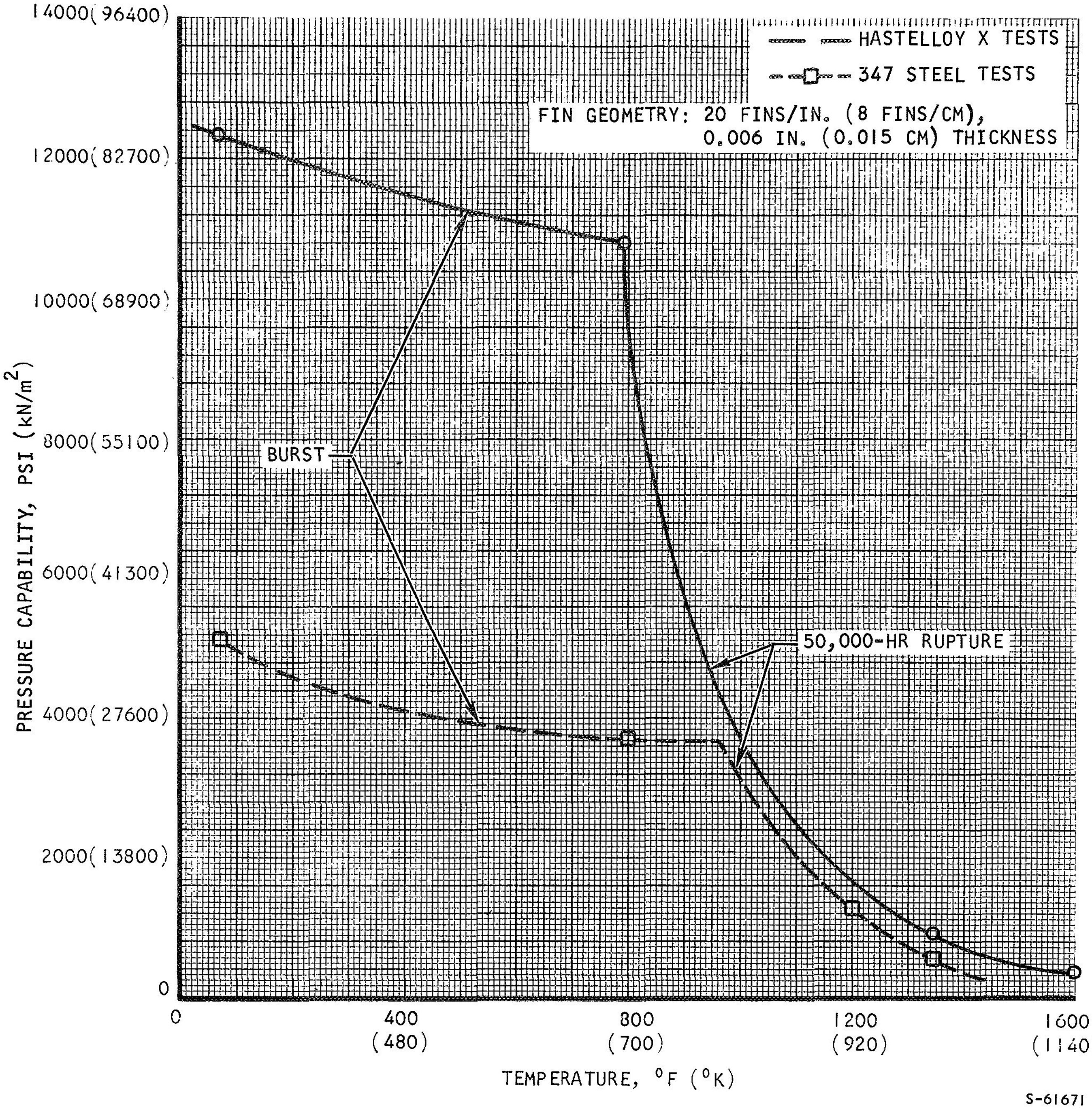

Figure 5-1. Typical Plate-Fin Pressure Capability vs Temperature for 347 Stainless Steel Brazed with AMS 7-4778 and Hastelloy X Brazed with Palniro I

BURST TESTS

The burst tests (Table 5-1) indicate that the 347 stainless steel specimens brazed with Palniro I were about 17 percent stronger than those brazed with AMS 7-4778. For the Hastelloy X specimens, the Palniro I braze alloy gave burst pressures which were an average of 28 percent higher than the AMS 7-4778 alloy. The Hastelloy X burst pressures were 61 to 83 percent of the theoretical value based on parent metal ultimate tensile strength whereas the 347 stainless steel specimens had 41 to 50 percent of the theoretical value. This disparity in burst strength ratios for the same fin spacing and thickness is not understood. However, it may be due to reductions in 347 stainless steel ultimate tensile stress resulting from the brazing process. Hastelloy X burst strength was an average of more than a factor of two higher than 347 stainless steel, indicating a considerable weight advantage for Hastelloy X for burst pressure limited designs where minimum gauge limitations are not a factor.

The observed strength reductions due to the temperature increase from room temperature to 800°F (700°K) compare favorably with published parent metal behavior. This is to be expected if the fin stress level is a reasonable correlation to the plate-fin burst pressure of Equation (5-2).

CREEP TESTS

The creep rupture results in Table 5-2 are presented on curves of internal pressure vs time-to-rupture in Figures 5-2 through 5-5. The predicted pressure capability from average parent metal creep data are also shown using Equation (5-1). The average line for the test data is drawn parallel to the published property curve since in some cases the range of rupture life values is limited. Where the range of test data extends over a factor of 100 on life, the test data gives a slope comparable to the parent metal slope, indicating that this is a reasonable assumption.

The strength ratios quoted in Table 5-2 were obtained from Figures 5-2 through 5-5. The 347 stainless steel brazed with AMS 7-4778 had a ratio of 0.81 to 0.85; this was considerably higher than the other specimens which ranged from 0.51 to 0.62. This significant difference may be attributed to increased 347 stainless steel creep strength resulting from the AMS 7-4778 braze cycle and braze alloying effects. The ratios between plate-fin and theoretical fin strength were generally comparable at the two test temperatures for each alloy combination with the exception of the Hastelloy X specimens brazed with AMS 7-4778. These specimens exhibited a loss in strength relative to parent metal properties at 1600°F (1140°K) as compared to the 1350°F (1010°K) test temperature. This may be attributed to corrosion which would be expected for the nickel-base braze alloy in the air environment of the furnace. (Several of the Hastelloy X-AMS 7-4778 specimens failed at the joint between the sheet and header bar which is exposed to the furnace environment.)

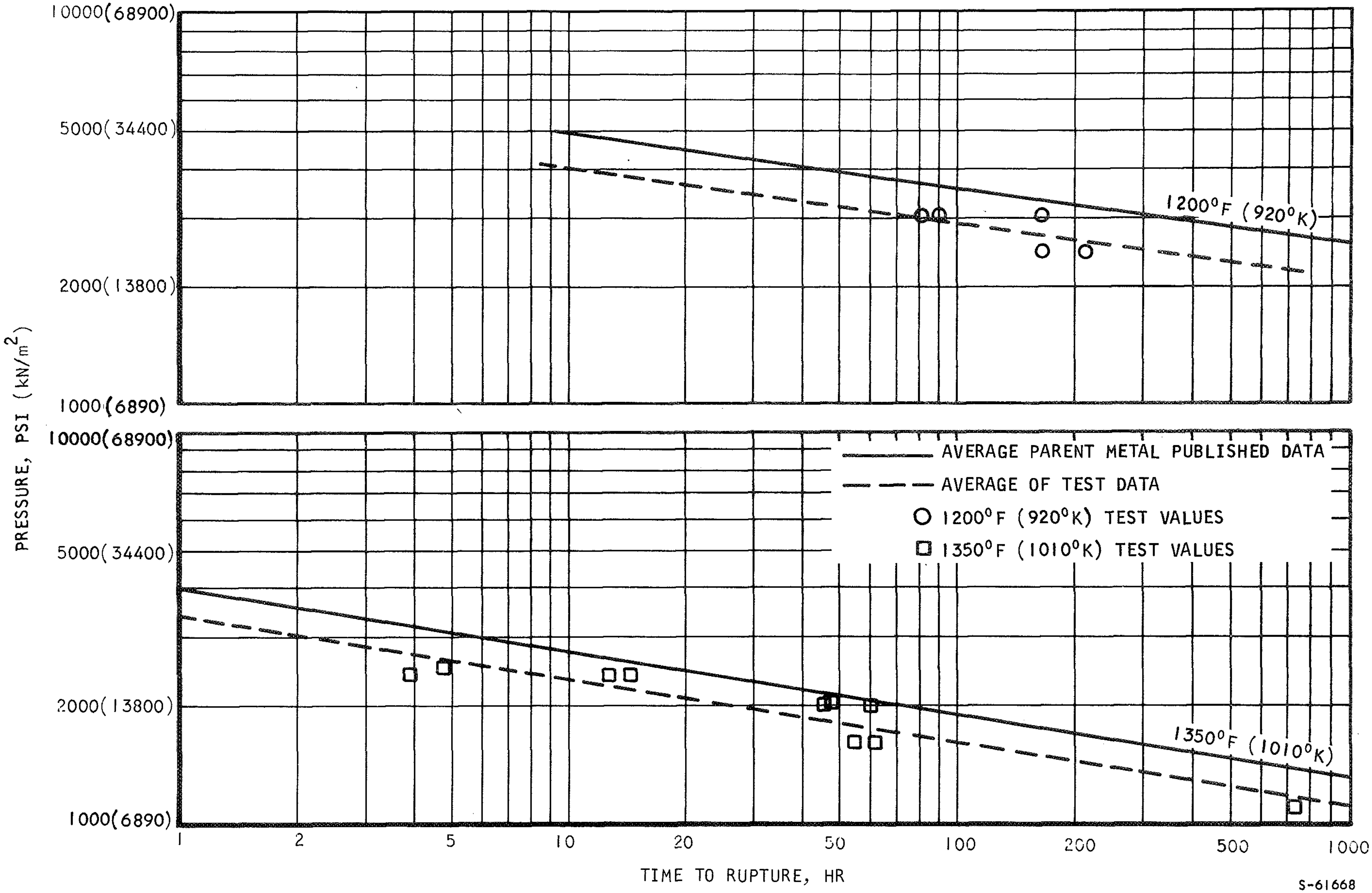

Figure 5-2. Creep Strength of 347 Stainless Steel Brazed with AMS 7-4778

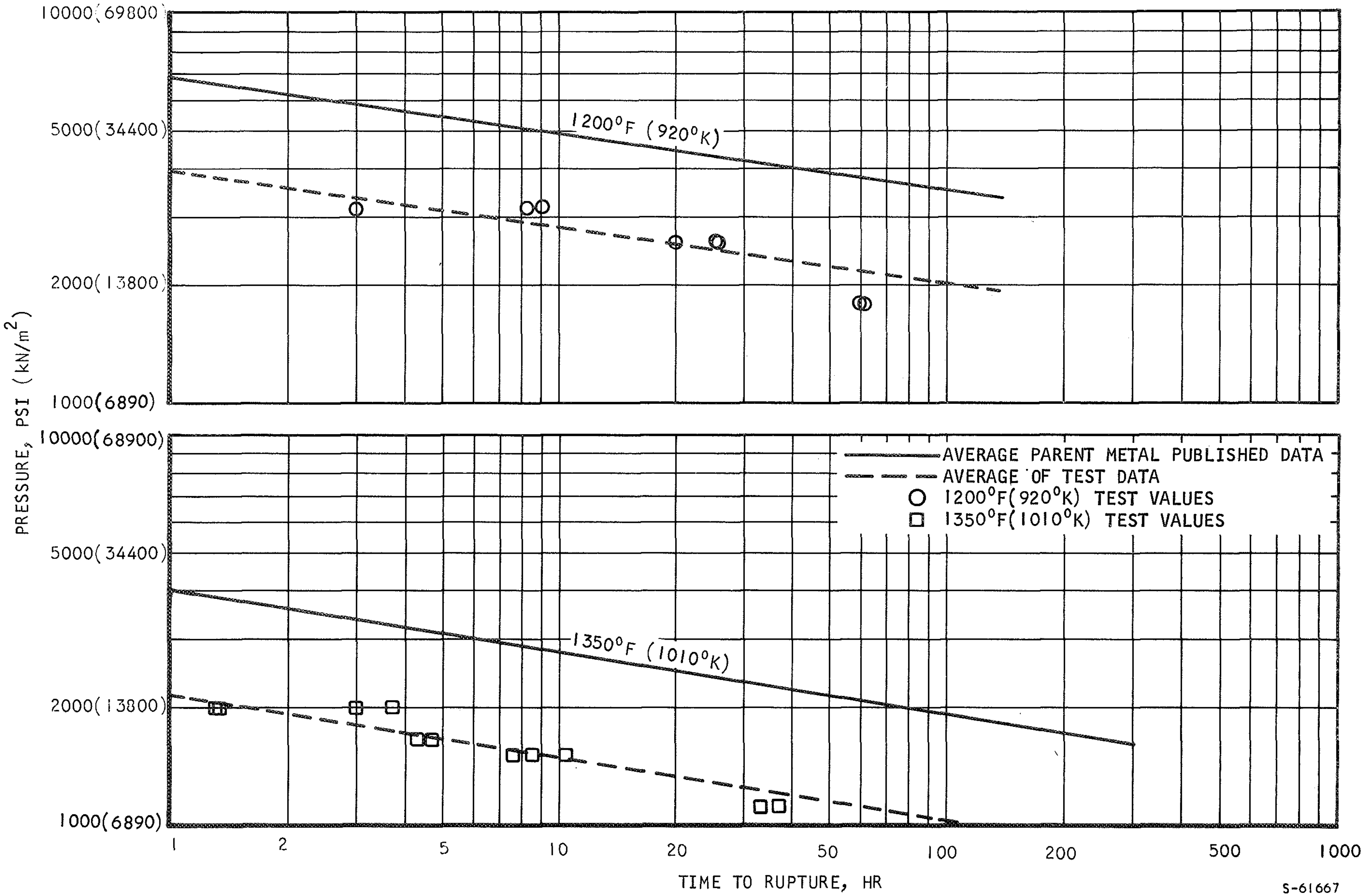

Figure 5-3. Creep Strength of 347 Stainless Steel Brazed with Palniro I

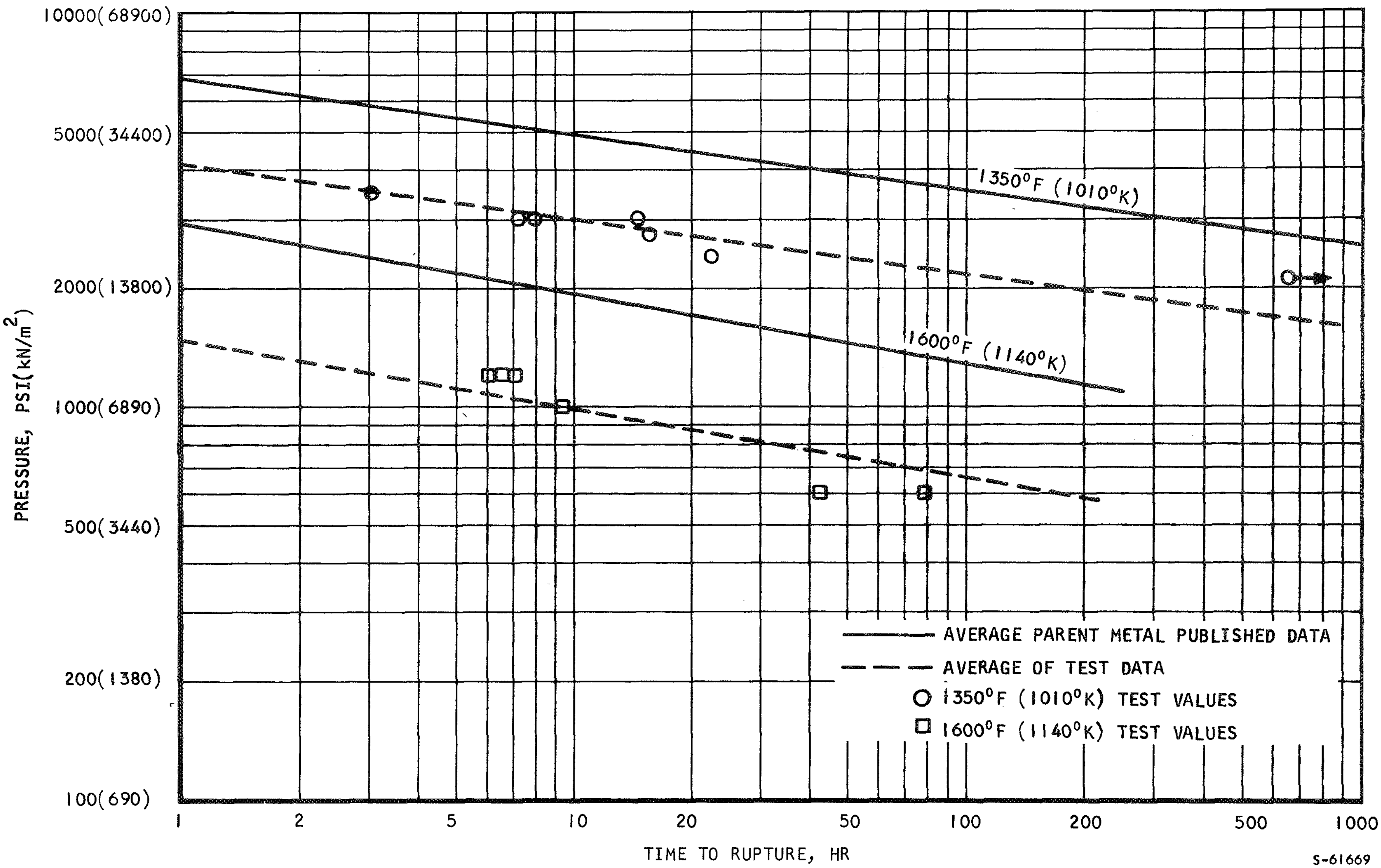

Figure 5-4. Creep Strength of Hastelloy X Brazed with AMS 7-4778

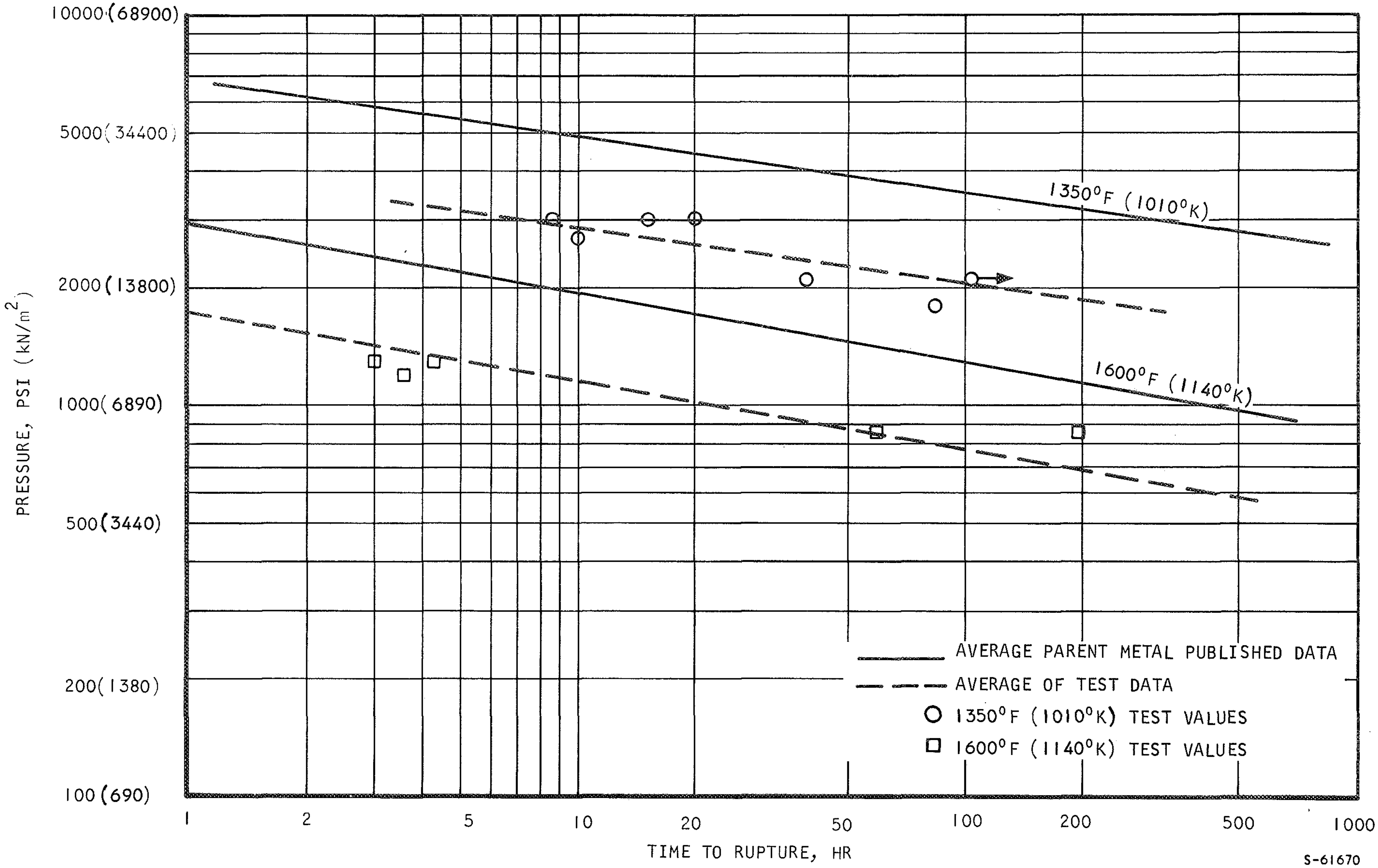

Figure 5-5. Creep Strength of Hastelloy X Brazed with Palniro I

The pressure capability of the four specimen types at 1350°F (1010°K) is compared in Figure 5-6. The average test lines, taken from Figure 5-2 through 5-5, show that Hastelloy X brazed with AMS 7-4778 was the strongest specimen, although the Hastelloy X-Palniro I and 347 stainless steel-AMS 7-4778 types had comparable pressure capability. The 347 stainless steel brazed with Palniro I had about 50 percent of the pressure capability of the other combinations. Although Hastelloy X brazed with AMS 7-4778 had the highest strength at 1350°F (1010°K), the corrosion resistance of the Palniro I alloy would presumably make it the preferred alloy combination for temperatures in the 1300° to 1600°F (980 to 1140°K) operating temperature range.

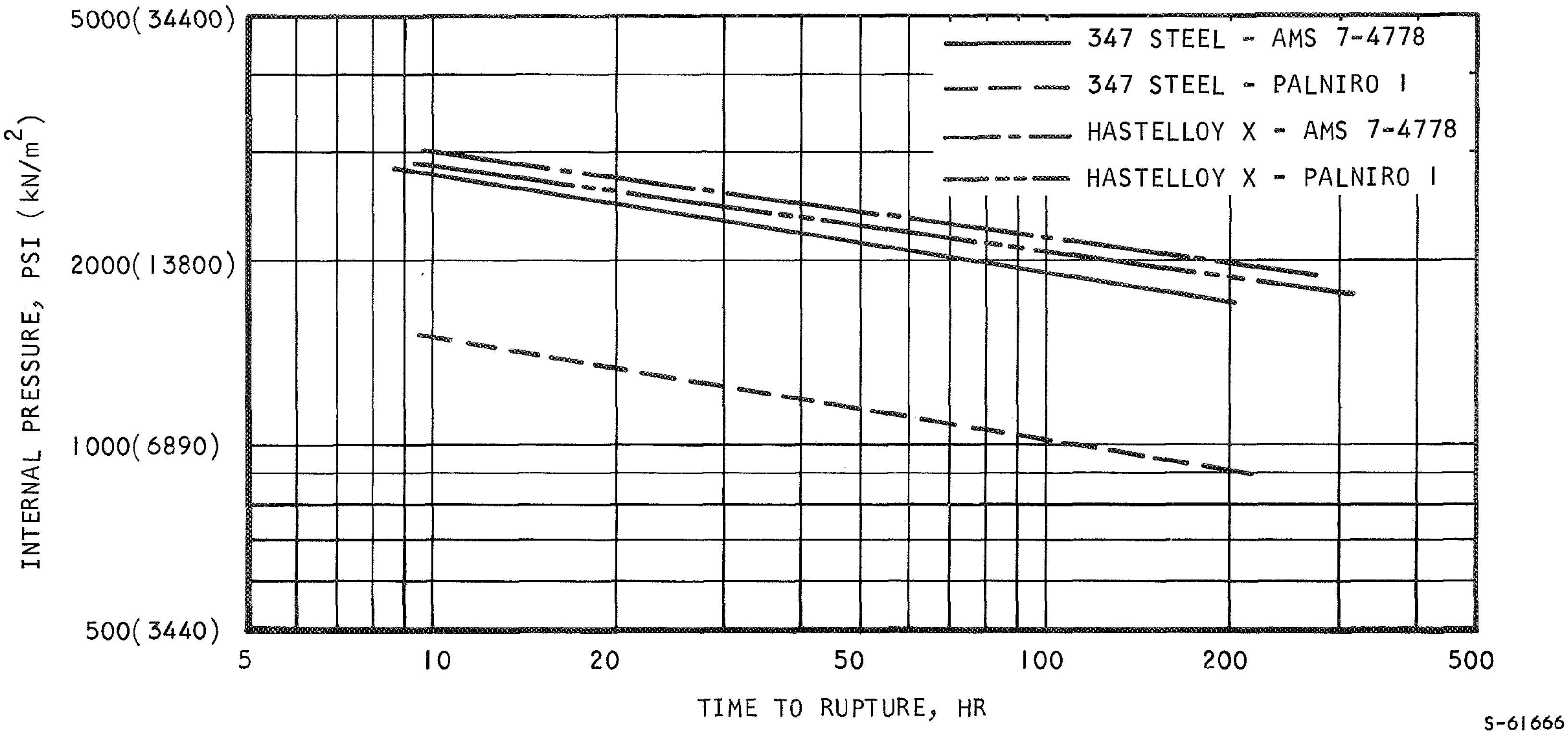

Figure 5-6. Comparative Creep Test Results at 1350°F (1010°K)

SECTION 6

REFERENCES

1. Coombs, M. G.; Morse, C. J.; and Richard, C. E.: Conceptual Design Study of Nuclear Brayton Cycle Heat Exchanger and Duct Assembly (HXDA). NASA CR-72783, December 4, 1970.

2. Coombs, M. G.; Morse, C. J.; and Richard, C. E.: Preliminary Design Study of Nuclear Brayton Cycle Heat Exchanger and Duct Assembly (HXDA). NASA CR-72716, January 4, 1970.

3. Anon: Steels for Elevated Temperature Service. ADUSS 43-1089, United States Steel, 1965.

4. Anon: Hastelloy alloy X. Report F-30,037-D, Union Carbide Corporation, October 1964.

DISTRIBUTION LIST

NASA-Lewis Research Center
21000 Brookpark Road
Cleveland, Ohio 44135
Attention: (See list below)
- G. M. Ault (MS 3-13) - 1
- R. E. English (MS 500-201) - 1
- H. O. Slone (MS 500-201) - 1
- J. A. Heller (MS 500-201) - 1
- E. E. Kempke, Jr. (MS 500-201) - 1
- J. P. Joyce (MS 500-201) - 1

- D. C. Guentert (MS 500-201) - 1
- D. R. Packe (MS 500-201) - 1
- D. G. Beremand (MS 500-201) - 1
- W. T. Wintucky (MS 500-201) - 1
- R. R. Miller (MS 500-202) - 1
- M. J. Saari (MS 500-202) - 1

- P. A. Thollot (MS 500-201) - 1
- W. L. Stewart (MS 77-2) - 1
- P. T. Kerwin (MS 500-201) - 53
- G. M. Thur (MS 500-202) - 1
- S. J. Kaufman (MS 49-2) - 1
- V. F. Hlavin (MS 3-14) - 1

- J. E. Dilley (MS 500-309) - 1
- Technology Utilization (MS 3-19) - 1
- Report Control (MS 5-5) - 1
- Reliability & Quality Assurance (MS 500-111) - 1
- Library (MS 60-3) - 2
- R. L. Johnsen (MS 500-201) - 1

NASA-Lewis Research Center
Plum Brook Station
Sandusky, Ohio 44870
Attention: D. B. Fenn (MS 1441-1) - 2

National Aeronautics &
Space Administration
Washington, D.C. 20546
Attention: (See list below)
- RNP/P. R. Miller - 1
- RNP/H. D. Rochen - 1
- RNT/J. Lazar - 1

NASA Scientific & Technical Information
P. O. Box 33
College Park, Maryland 20740
Attention: Acquisitions Branch (SQT-34054) - 1

NASA-Marshall Space Flight Center
Marshall Space Flight Center, Alabama 35812
Attention: (See list below)
- Library - 1
- C. Graff - 1
- W. Brantley - 1

NASA-Flight Research Center
P. O. Box 273
Edwards, California 93523
Attention: Library - 1

NASA-Ames Research Center
Moffitt Field, California 94035
Attention: Library - 1

NASA-Goddard Space Flight Center
Greenbelt, Maryland 20771
Attention: Library - 1

NASA-Langley Research Center
Langley Station
Hampton, Virginia 23365
Attention: Library - 1

Jet Propulsion Laboratory
4800 Oak Grove Drive
Pasadena, California 91103
Attention: Library - 1

NASA-Manned Spacecraft Center
Houston, Texas 77058
Attention: (See list below)
- Library - 1
- A. Redding - 1
- J. Grayson - 1

AEC Headquarters
Space Nuclear Systems Division
Germantown, Maryland 20545
Attention: C. Johnson - 2

Air Force Systems Command
Aeronautical Systems Division
Wright-Patterson Air Force Base,
Ohio 45438
Attention: Library - 1

U.S. Army Engineer R&D Labs
Gas Turbine Test Facility
Fort Belvoir, Virginia 22060
Attention: W. Crim - 1

Bureau of Naval Weapons
Department of the Navy
Washington, D.C. 20025
Attention: Code RAPP - 1

Institute for Defense Analyses
400 Army-Navy Drive
Arlington, Virginia 22202
Attention: Library - 1

Office of Naval Research
Department of the Navy
Washington, D. C. 20025
Attention: Dr. Ralph Roberts - 1

Naval Facilities Engineering Command
P. O. Box 610
Falls Church, Virginia 22046
Attention: Graham Heggy, Code 042 - 1

Bureau of Ships
Department of the Navy
Washington, D. C. 20025
Attention: L. Graves - 1

University of Virginia
School of Engineering & Applied Science
Dept. of Mechanical Engineering
Charlottesville, Virginia 22903
Attention: Dr. E. J. Gunter, Jr. - 1

University of Maryland
College of Engineering
College Park, Maryland 20740
Attention: M. E. Talast - 1

Massachusetts Institute of Technology
Cambridge, Massachusetts 02139
Attention: Library - 1

Battelle Memorial Institute
505 King Avenue
Columbus, Ohio 43201
Attention: Library - 1

Power Information Center
University of Pennsylvania
3401 Market Street, Room 2107
Philadelphia, Pennsylvania 19104

Aerospace Corporation
2350 East El Segundo Blvd.
El Segundo, California 90045
Attention: H. T. Sampson - 1

AVCO-Bay State Abrasives Division
Westboro, Massachusetts 01581
Attention: George Herterick - 1

Aerojet-General Corporation
Von Karman Center
Azusa, California 91702
Attention: Library - 1

Bendix Research Labs. Division
Detroit, Michigan 48232
Attention: Library - 1

Borg-Warner Corporation
Pesco Products Division
24700 North Miles Road
Bedford, Ohio 44014
Attention: Library - 1

Continental Aviation & Engineering Corporation
12700 Kercheval Avenue
Detroit, Michigan 48215
Attention: Library - 1

The Boeing Company
Aero-Space Division
Box 3707
Seattle, Washington 98124
Attention: Library - 1

Curtiss-Wright Corporation
Wright Aero Division
Main and Passaic Streets
Woodridge, New Jersey 07075
Attention: Library - 1

Consolidated Controls Corp.
15 Durant Avenue
Bethel, Connecticut 06801
Attention: Library - 1

Garrett Corporation
AiResearch Manufacturing Company
402 South 36 Street
Phoenix, Arizona 85034
Attention: R. A. Rackley - 2

Garrett Corporation
AiResearch Manufacturing Company
9851 Sepulveda Blvd.
Los Angeles, California 90009
Attention: M. G. Coombs - 1

General Dynamics Corporation
16501 Brookpark Road
Cleveland, Ohio 44142
Attention: Library - 1

General Electric Company
Missile & Space Vehicle Dept.
3198 Chestnut Street
Philadelphia, Pennsylvania 19104
Attention: Library - 1

General Electric Company
Lynn, Massachusetts 01905
Attention: Library - 1

General Electric Company
Mechanical Technology Laboratory
R&D Center
Schnectady, New York 12301
Attention: Library - 1

General Electric Company
Flight Propulsion Laboratory Div.
Cincinnati, Ohio 45215
Attention: Library - 1

General Motors Corporation
Indianapolis, Indiana 46206
Attention: Library - 1

Franklin Institute Research Laboratories
Benjamin Franklin Parkway at 20th Street
Philadelphia, Pennsylvania 19103
Attention: Library - 1

General Electric Company
Missile and Space Division
Cincinnati, Ohio 45215
Attention: D. Huebner - 2

Lear Siegler, Inc.
3171 S. Bundy Drive
Santa Monica, California 90406
Attention: Library - 1

Lockheed Missiles & Space Co.
P.O. Box 504
Sunnyvale, California 94088
Attention: Library - 1

McDonnell-Douglas Corporation
Space Station Office
Huntington Beach, California
Attention: R. Gervais - 2

McDonnell-Douglas Corporation
Lambert Field
St. Louis, Missouri 63166
Attention: Library - 1

North American Rockwell Corp.
Space Division
12214 Lakewood Blvd.
Downey, California
Attention: (See list below)

- A. Nusseberger - 1
- C. Gould - 1
- W. Schmill - 1

North American Rockwell
Atomics International Division
P. O. Box 309
8900 DeSota Avenue
Canoga Park, California 91304
Attention: (See list below)

- T. A. Moss - 1
- W. Botts - 1

Northern Research & Engineering Co.
219 Vassar Street
Cambridge, Massachusetts 02139
Attention: Library - 1

Mechanical Technology Inc.
968 Albany-Shaker Road
Latham, New York 12110
Attention: Library - 2

Solar Division of International Harvester
2200 Pacific Highway
San Diego, California 92112
Attention: Library - 1

Sunstrand Denver
2480 West 70 Avenue
Denver, Colorado 80221
Attention: Library - 1

TRW Systems Division
One Space Park
Redondo Beach, California 90278
Attention: Library - 1

Union Carbide Corporation
Linde Division
P. O. Box 44
Tonawanda, New York 14152
Attention: Library - 1

United Aircraft Corporation
Pratt & Whitney Aircraft
West Palm Beach, Florida 33402
Attention: Dr. R. A. Schmidtke - 1

United Aircraft Research Lab.
East Hartford, Connecticut 06108
Attention: Library - 1

Westinghouse Electric Corporation
Aerospace Electrical Division
P. O. Box 989
Lima, Ohio 45802
Attention: A. King - 1

Westinghouse Electric Corporation
Astronuclear Laboratory
P. O. Box 10864
Pittsburth, Pennsylvania 15236
Attention: Library - 1

Williams Research
Walled Lake, Michigan 48088
Attention: Library - 1

Naval Ship Engineering Center
Hyattsville, Maryland 20782
Attention: Frank Welling - 2

TRW, Inc.
23555 Euclid Avenue
Euclid, Ohio 44117
Attention: Bill Davis - 1